COPPER-CARBON NANOCOMPOSITES BASED ON SYNTHETIC HUMIC SUBSTANCES

Valentina A. Litvin[1,*] Roger Abi Njoh[2]

[1]*Bohdan Khmelnitsky National University, Shevchenko str. 81, Cherkasy, 18031, Ukraine*
[2]*Near East University, Near East boulevard, 99138 Nicosia, Cyprus*

Abstract

A new method for the synthesis of copper-carbon nanocomposite using synthetic humic substances as a carbon source is presented. The method is based on the pyrolysis of copper (II) humate in a reducing (H_2) and inert (Ar) atmosphere. The structure and properties of the Cu/C nanocomposites were characterized by X-ray diffraction (XRD), FT-IR spectroscopy, transmission electron microscopy (TEM), elemental analysis. The porous structure of Cu/C nanocomposite was investigated by nitrogen volumetric adsorption. Under the conditions of the synthesis, a carbon matrix with a very low degree of order is formed. It was found that the dimensional and structural characteristics of the copper nanoparticles depend on the synthesis conditions and vary from 40 to 80 nm. Carrying out the synthesis in a reducing atmosphere makes it possible to obtain the copper-carbon nanocomposites that do not contain copper (I) oxide or copper (II) oxide phases. It was found out that an increase in the pyrolysis temperature contributes to an improvement of the metal phase crystal lattice structure, an increase in the degree of the organic component carbonization, and a change in the textural characteristics from mesoporous to microporous.

Keywords: nano-structures; copper-carbon nanocomposites; synthetic humic substances.

МІДЬ-КАРБОНОВІ НАНОКОМПОЗИТИ НА ОСНОВІ СИНТЕТИЧНИХ ГУМІНОВИХ РЕЧОВИН

Валентина А. Литвин,[1] Роджер Абі Нйо[2]

[1]*Черкаський національний університет ім. Б. Хмельницького, бульв. Шевченка, 81, Черкаси, 18031, Україна*
[2]*Близькосхідний університет, Близькосхідний бульвар, Нікосія, 99138, Кіпр*

Анотація

Розроблено нову методику синтезу мідь-карбонового нанокомпозиту з використанням синтетичних гумінових речовин як джерела Карбону. В основу методики покладено піроліз купрум (II) гумату, який проводили як у відновлюючій водневій, так і інертній атмосфері. Структуру та властивості Cu/C нанокомпозиту охарактеризовано методом рентгенівської дифракції, ІЧ-спектроскопії, просвічуючої електронної мікроскопії, елементного аналізу. Пористу структуру Cu/C нанокомпозиту досліджено методом об'ємної адсорбції азоту. В умовах синтезу формується карбонова матриця з дуже низьким ступенем впорядкованості. Встановлено, що розмірні та структурні харакеристики наночастинок міді залежать від умов синтезу і варіюються від 40 до 80 нм. Проведення синтезу у відновній атмосфері дозволяє одержати мідь-вуглецеві нанокомпозити, що не містять фази купрум (I) оксиду або купрум (II) оксиду. Встановлено, що підвищення температури піролізу сприяє вдосконаленню будови кристалічної ґратки металічної фази, підвищенню ступеня карбонізації органічної складової та зміні текстурних характеристик від мезопористих до мікропористих.

Ключові слова: наноструктури; мідь-карбонові нанокомпозити; синтетичні гумінові речовини.

МЕДЬ-УГЛЕРОДНЫЕ НАНОКОМПОЗИТЫ НА ОСНОВЕ СИНТЕТИЧЕСКИХ ГУМИНОВЫХ ВЕЩЕСТВ

Валентина А. Литвин,[1] Роджер Аби Нйо[2]

[1]Черкасский национальный университет им. Б. Хмельницкого, бульв. Шевченка, 81, Черкассы, 18031, Украина
[2]Ближневосточный университет, Ближневосточный бульвар, Никосия, 99138, Кипр

Аннотация

Разработана новая методика синтеза медь-углеродного нанокомпозита с использованием синтетических гуминовых веществ как источника углерода. В основу методики положен пиролиз купрум (II) гумата, который проводили как в восстановительной водородной, так и инертной атмосфере. Структура и свойства Cu/C нанокомпозита охарактеризованы методом рентгеновской дифракции, ИК-спектроскопии, просвечивающей электронной микроскопии, элементного анализа. Пористую структуру Cu/C нанокомпозита исследовано методом объемной адсорбции азота. В условиях синтеза формируется карбоновая матрица с очень низкой степенью упорядоченности. Установлено, что размерные и структурные харакеристики наночастиц меди зависят от условий синтеза и варьируются от 40 до 80 нм. Проведение синтеза в восстановительной атмосфере позволяет получить медь-углеродные нанокомпозиты, не содержащие фазы купрум (I) оксида или купрум (II) оксида. Установлено, что повышение температуры пиролиза способствует совершенствованию строения кристаллической решетки металлической фазы, повышению степени карбонизации органической составляющей и изменении текстурных характеристик от мезопористых к микропористым.

Ключевые слова: наноструктуры; медь-углеродные нанокомпозиты; синтетические гуминовые вещества.

Introduction

Metal/carbon nanocomposites are nanostructures containing metal nanopartiсles stabilized by a carbon shell. As a result of the stabilization of metal particles by the carbon phase, chemically active metal particles are stable in air and when heated [1–3]. The association of the metal phase and the carbon component gives the composite unique properties, which are currently the subject of intense research.

The specific physical and chemical properties of Cu/C nanocomposites determine their wide application in catalytic [4; 5], optical [6], sensory [7] and electronic devices [8]. In addition, copper nanoparticles have antibacterial properties [9; 10] and are an alternative to more expensive silver nanoparticles in medicine.

Obtaining nanostructured metal-carbon composites that are pure, regularly constructed, with specified functional properties, morphology, and composition is a complex multi-stage process. The most common methods for obtaining metal nanoparticles on the surface of a carbon matrix are vapor deposition (CVD), pyrolysis, electron beam exposure, chemical reduction with ultrasonic stabilization, and carbonization [11–15].

One of the practically important methods of obtaining metal-carbon nanostructured materials is the thermal decomposition of organometallic precursors of various nature in a hydrogen flow. An important fundamental problem, the solution of which opens up the possibility of controlling the structure of nanocomposites, is the study of the dependence of the metal particles size and the metal-carbon nanocomposites structural characteristics on the conditions of their preparation.

In this work we present a method for the preparation of Cu/C nanocompozites via the carbonization of a copper-containing precursor obtained by the interaction of $CuSO_4$ with synthetic humic substances. By using synthetic humic substances as a source of carbon, we expect to obtain a nanocomposite material with the regular distribution of Cu nanoparticles in the carbon support. In contrast to the traditional precursors, synthetic humic substances carbonize during pyrolysis without melting the sample with the formation of a minimal amount of by-products. During the pyrolysis of humic substances in a hydrogen atmosphere, one can hope to obtain amorphous carbon of high purity. The effect of thermal decomposition conditions on the structure and sorption properties of Cu/C nanocomposites was studied.

Experimental part

Tannin (99 % purity, analytical grade) was purchased from Sigma Aldrich (Germany). Other chemicals were of analytical grade (Merck, Germany). Deionized water from Milli-Q system (Millipore) was used for all the samples preparation and dilutions.

The precursor in the synthesis of copper-carbon nanocomposite was synthetic copper humate. The copper humate was obtained from humic substances synthesized according to the method described in [16]. 100 ml of the solution containing 1.5 g of synthetic humic substances was neutralized with alkali to pH = 11. 10 ml of 1 M $CuSO_4$ solution was added to the resulting solution. The precipitate was washed by the decantation, filtered and dried at 120 °C. The pyrolysis of dried copper (II) humate was

performed in a hydrogen atmosphere in the temperature range of 300–900–°C. In each experiment the weight loss of the original copper(II) humate was determined by weighing the crucible with the substance before and after the pyrolysis with an accuracy of 0.0001 g. The pyrolysis time was 1 h from the moment of reaching the nominal temperature. The reactor tube was also cooled to the room temperature by passing hydrogen through the system.

The phase and crystal structures of Cu/C nanocomposites were characterized using X-Ray diffraction (Bruker D8 Advance) with CuKα radiation (λ = 1.54184 Å). The measurements were performed in a 2θ range of 10–90° with a scanning step 0.03° and exposure time 5 s/step. The average crystallite size of the copper nanoparticles was estimated using the Scherrer equation:

$$D = \frac{k \cdot \lambda}{\beta \cdot \cos\theta},$$

where the value of D – the size of the crystallites, λ – the wavelength of radiation, θ – the Bragg diffraction angle and β – the intrinsic (true) profile full width at half maximum intensity.

The FT-IR spectra of the samples were recorded by the Perkin Elmer Spectrum One Fourier spectrometer with a resolution of 2 cm^{-1} over a scanning range 4000–400 cm^{-1} using KBr pellet method. The tablet samples were made by pressing the Cu/C nanocomposites with KBr in a ratio of 0.7–1 mg, 70–100 mg, respectively. The tablets were pressed under a pressure of 10 MPa. The preparation of samples in this way made it possible to obtain informative spectra. IR spectra were recorded using a Perkin Elmer Spectrum One Fourier spectrometer.

The photomicrographs were recorded on a SELMI TEM-125K transmission electron microscope at an accelerating voltage of 100 kV. The samples for the TEM study were grounded in an agate mortar with alcohol. The resulting suspension was applied to a copper mesh covered with a carbon film.

The adsorption-desorption isotherms of nitrogen with a purity of 99.99 % were measured by the volumetric method at 77 K and atmospheric pressure (~ 760 torr) using Sorptomatic 1990. The specific surface area (SBET) was estimated using the BET (Brunauer-Emmett-Teller) equation [17]. The micropore size was calculated using Horvath Kavazoe equation [18]. The micropore volume in obtained Cu/C nanocomposites was calculated using t-plot method [17].

Results and discussion

Synthetic humic substances are polyfunctional compounds containing carboxyl, hydroxyl and carbonyl groups in which they form insoluble salts with multiply charged metal cations [19]. In addition, the polyfunctionality of synthetic humic substances allows metal ions to be evenly distributed over the organic matter [20]. Similarly, adding an excess of copper (II) sulfate to an alkaline solution of synthetic humic substances leads to the formation of a brown precipitate of copper (II) humate, which, according to X-ray phase analysis, has an amorphous structure. Heating in the hydrogen atmosphere leads to the decomposition of the formed precipitate. In the hydrogen atmosphere, copper (II) cations are reduced to the zero-valence state and metal nanoparticles grow. The thermal decomposition of the humic residue leads to the formation of a carbon matrix, which contains reduced copper nanoparticles. The thermal decomposition of copper(II) humate in an inert atmosphere similarly leads to the reduction of copper and the formation of a copper-carbon nanocomposite.

Fig. 1 shows the IR spectra of the synthetic humic substances, washed and dried precipitate of copper (II) humate and the Cu/C nanocomposite. The position of the main absorption bands in the IR spectra of copper (II) humate corresponds with the initial humic substances, but is not observed in the IR spectra of the Cu/C nanocomposite. The latter is due to the decomposition of the organic part of the complex during the pyrolysis reaction and its carbonization. The detailed analysis of the IR spectra makes it possible to establish the formation of the corresponding intermediate products at various stages of the nanocomposite preparation process.
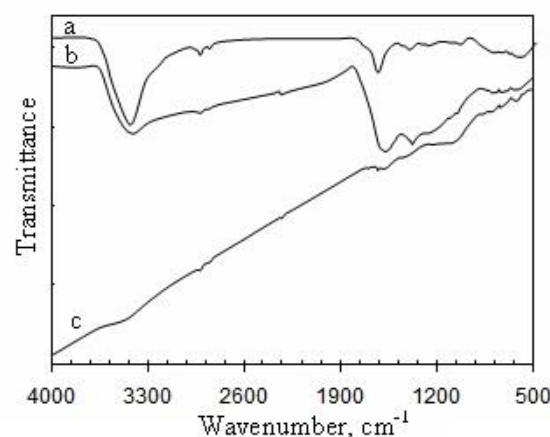

Fig. 1. IR spectra of synthetic humic substances (a), copper(II) humate (c), Cu/C nanocomposite obtained at 300 °C in H$_2$ atmosphere (c).

The IR spectra of all the compounds exhibit a broad band at about 3400 cm⁻¹, which corresponds to the vibrations of hydroxyl groups both in the organic part of the complex and in water molecules. Two bands at frequencies of 2927 cm⁻¹ and 2846 cm⁻¹, that correspond to the stretching vibrations of the C - H bond in CH_2 and CH_3 groups, are also observed in the spectra of the starting humic substances and copper (II) humate, but are practically absent in the spectrum of the product. The absorption bands of the stretching vibration of the C = O group at 1750–1730 cm⁻¹, that are characteristic of humic substances [20; 21], are poorly expressed in the IR spectrum of humic substances. This is due to the overlap of this band with a wide intense absorption band of water molecules deformation vibrations at 1600 cm⁻¹. In the spectrum of copper (II) humate, the absorption band of the C = O group has even lower intensity, which is typical for the salts of humic substances [21]. In the IR spectrum of the Cu/C nanocomposite, vibrations of the C = O group are not observed due to their elimination during thermal transformation. But in these ranges, there is an absorption band at 1084 cm⁻¹, which is similar to the stretching vibration of the Cu–C bond in copper (I) acetelenides [22]. The absorption in the region of about 1400 cm⁻¹, observed in the IR spectra of humic substances and copper (II) humate, may be due to the bending vibrations of the OH group and stretching vibrations of the C-O in phenolic OH groups, as well as the bending vibrations of the CH in CH_2 or CH_3 groups [21; 22].

Based on the analysis of IR spectra, it can be concluded that the carbonization of the organic part of copper (II) humate is high as a result of pyrolysis, resulting in the formation of a carbonaceous substrate of nanocomposites.

The influence of the synthesis conditions was studied by reducing copper (II) humate in an inert and reducing atmosphere at different temperatures. Heating was performed in the temperature range from 300 to 900 °C. The samples obtained by decomposition of copper (II) humate in a hydrogen and argon atmosphere at different temperatures were marked Cu/C-H_2-t and Cu/C-Ar-t, respectively, where t corresponds to the temperature of the decomposition reaction.

On the diffraction pattern of the Cu/C nanocomposite (Fig. 2) obtained by reduction of copper (II) humate in a hydrogen atmosphere, five clear reflexes are observed at 2θ = 43.4°, 50.8°, 74.4°, 90.0° and 95.2°. This corresponds to a face-centered cubic lattice of copper [23]. The reflexes

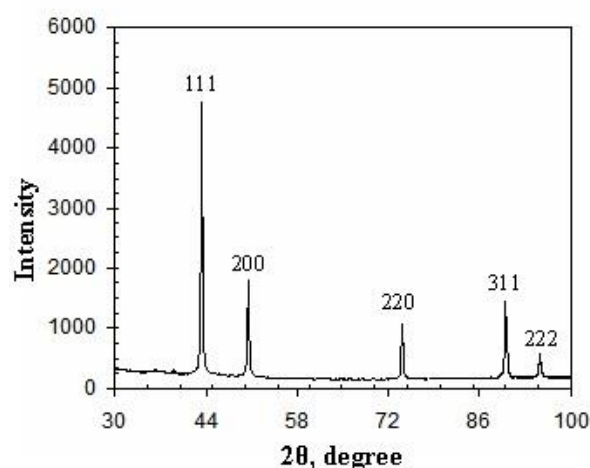are broad, which may indicate the nanocrystallinity of the sample.

Fig. 2. Diffraction pattern of the copper-carbon nanocomposite obtained in a hydrogen atmosphere at 300 °C

At the decomposition of copper (II) humate in an inert atmosphere, the reduction occurs due to the remainder of humic substances. This leads to the formation of metallic copper and copper (I) oxide. On the diffraction patterns of such samples, reflections from the fcc lattice of copper are observed (Fig. 3). In addition, the diffraction patterns have one intense reflection at 2θ = 36° and two low-intensity reflections at 2θ = 42°, 62°, corresponding to the copper (I) oxide phase. The broad peak in the range of angles 2θ = 20° ∼ 30°, which corresponds to amorphous carbon [24], has a low intensity and is hardly noticeable in the diffractograms of both composites.
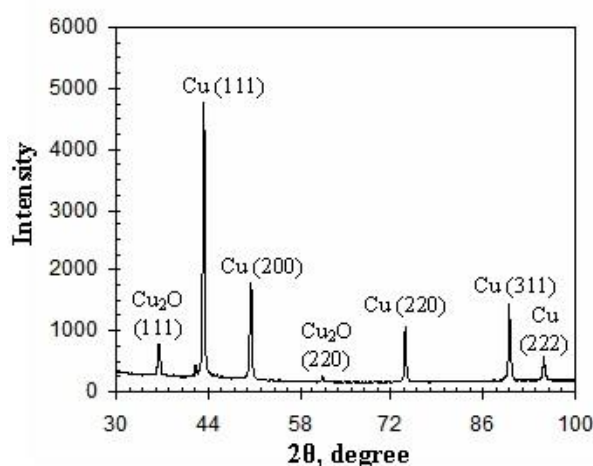

Fig. 3. Diffraction pattern of the copper-carbon nanocomposite obtained in inert atmosphere at 300 °C

Thus, pyrolysis of copper (II) humate in a reducing atmosphere makes it possible to obtain Cu/C nanocomposites that do not contain copper (I) oxide or copper (II) oxide phases within the sensitivity range of the diffractometric method.

It should be noted that carrying out thermal decomposition in an H_2 atmosphere makes it possible to obtain nanocomposites with the carbon content of about 50 %, while as a result of the reaction in an inert atmosphere, the carbon content is 35 %, since the reduction in this case occurs due to the organic part of the molecules. Therefore, carrying out the thermolysis reaction in a hydrogen atmosphere simultaneously ensures the complete reduction of metal cations to the zero-valent state and the maximum retention of the carbon.

At the temperatures above 300 °C, the carbonization processes develop in the residue of humic substances, which leads to the formation of a graphite-like structure with a low degree of order. According to the results of X-ray phase analysis on the diffractograms of the samples obtained in a reducing atmosphere, an amorphous halo is recorded in the range of angles $2\theta = 25$–$30°$, which is associated with the irregular displacement of the graphene planes relative to each other and the small size of the coherent scattering regions of the crystallites of the graphite-like phase (Fig. 4 c). In this case, there are no other reflection peaks. This indicates a low degree of carbon graphitization in nanocomposites and the formation of a turbostratic structure characteristic of amorphous carbon. With an increase in the pyrolysis temperature, the intensity of the peak increases (Fig. 4 c) due to an increase in the size of the crystallites of the graphite phase. However, even at the tpyrolysis temperature of 900 °C, the formation of a clearly pronounced graphite phase does not occur.
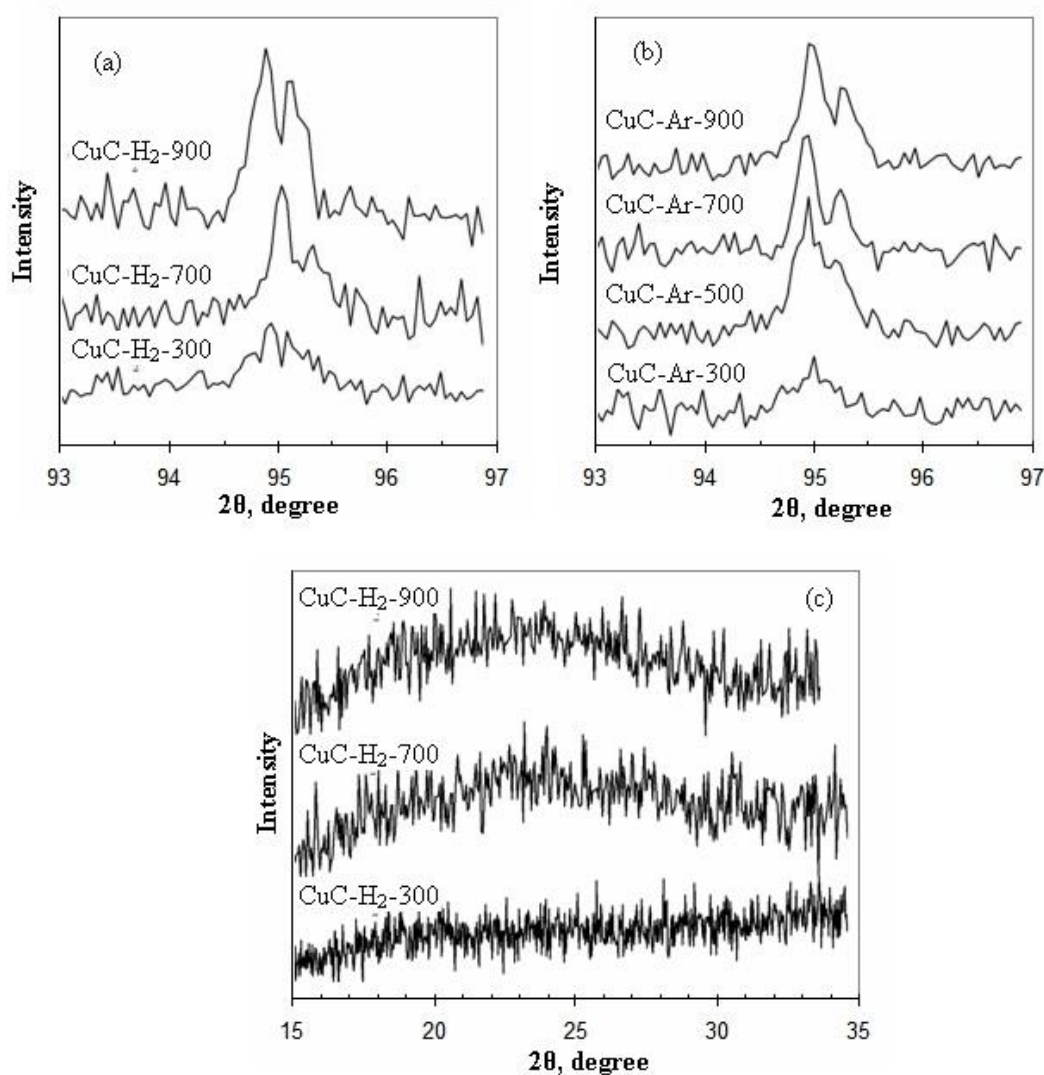

Fig. 4. Diffraction patterns of nanocomposites: large angular of intensity maxima (222) of the fcc lattice plane of copper in nanocomposites CuC-H₂-t (a) and CuC-Ar-t (b); the range of angles $2\theta = 15$–$35°$ (c)

The increase of the pyrolysis temperature does not change the lattice period of copper nanoparticles. However, the increase of the temperature contributes to the improvement of the crystal lattice structure of the metal phase, which is clearly seen by the change in the large-

angle intensity profile of fcc-Cu. Figures 4 a and 4 b show diffraction patterns in the region of large angles of fcc-Cu (222) for nanocomposites obtained at 300, 500, 700, and 900°C in a hydrogen and inert atmosphere, respectively. The increase of the pyrolysis temperature causes a decrease in the blurring of the maximum at the base, an increase in its intensity and the release of α-doublet. Such changes in the structure of fcc-Cu are obviously due to the processes of nucleation, growth, and relaxation of the structure of the metal phase. The increase in the reaction temperature leads to an increase of the growth rate and, accordingly, to an increase of the nanoparticles size. At the same time, the temperature factor contributes to the relaxation processes of the structure. A significant increase of the size of nanoparticles with the increasing pyrolysis temperature is not observed due to the limitation of the mobility of metal atoms in the carbon matrix.

The TEM study of the samples obtained in the atmosphere of H_2 showed that copper nanoparticles were distributed in a carbon matrix and had a spherical shape. The average sizes of copper nanoparticles and size distribution were calculated (Table 1, Fig. 6). The size of Cu nanoparticles in the CuC nanocomposites are in the range from 5 to 200 nm. At the same time, there are relatively few large metal inclusions, and most of them have a size of 40–80 nm
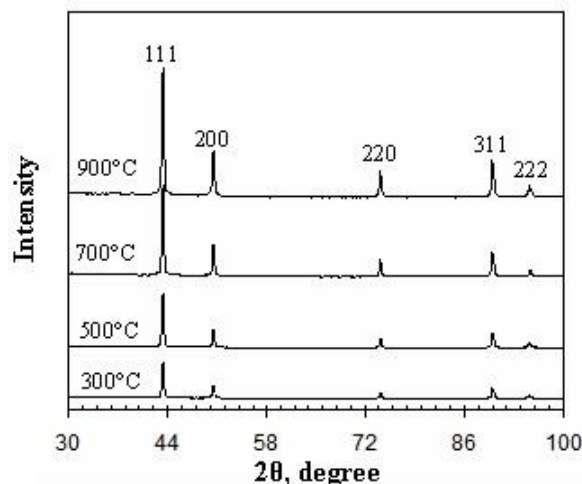

Fig. 5. Diffractograms of Cu/C nanocomposites obtained at different temperatures in a hydrogen atmosphere
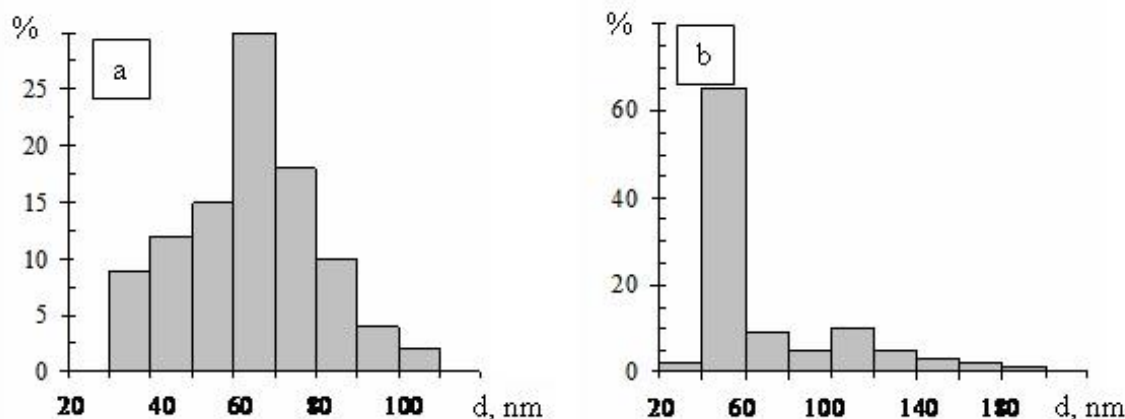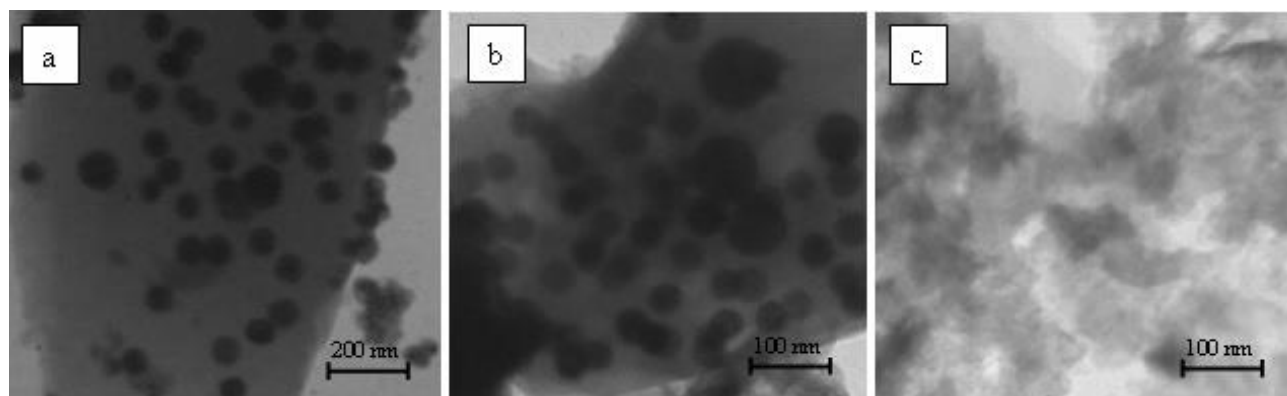

Fig. 6. Micrographs of samples nanocomposites CuC-H₂-300 (a), CuC-H₂-900 (b), CuC-Ar-900 (c) and histograms of nanoparticle size distribution

Table 1

Sizes of copper nanoparticles and crystal lattice parameters in Cu/C nanocomposites obtained at different temperatures in an atmosphere of H2

Sample	Sizes of nanocrystallites calculated by the Scherrer formula (± 1), nm	Lattice parameter (*a*), (± 0.01) Å	Sizes of nanocrystallites calculated by the TEM images, nm
Cu, bulk	-	3.6150	-
CuC-H2-300	33	3.6156	64
CuC-H2-500	36	3.6156	68
CuC-H2-700	45	3.6156	73
CuC-H2-900	47	3.6180	80

The wide particle size distribution can be due to the uneven distribution of Cu^{2+} cations in the organic fulvate matrix. Carrying out the reduction reaction in the solid phase complicates the migration of metal atoms during the formation and growth of nanoparticles, which also contributes to the formation of crystallites of different sizes.
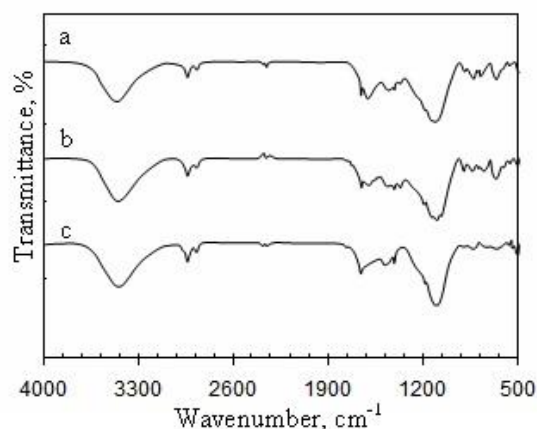
As a result of the pyrolysis in an inert atmosphere, poorly faceted nanoparticles are formed, which complicates their detection in micrographs (Fig. 6, c). Large dark areas in the images can correspond both to the aggregated nanoparticles and several overlapped layers of carbon.

The average sizes of nanoparticles calculated from the microscopic data differ from those calculated from the X-ray phase analysis data. This difference can be explained by the wide size distribution of nanoparticles. The presence of small nanoparticles affects the average size value calculated from the X-ray diffraction data. At the same time, the inclusion of nanoparticles in the carbon matrix reduces their contrast in micrographs, which interferes to the identification of small nanoparticles.
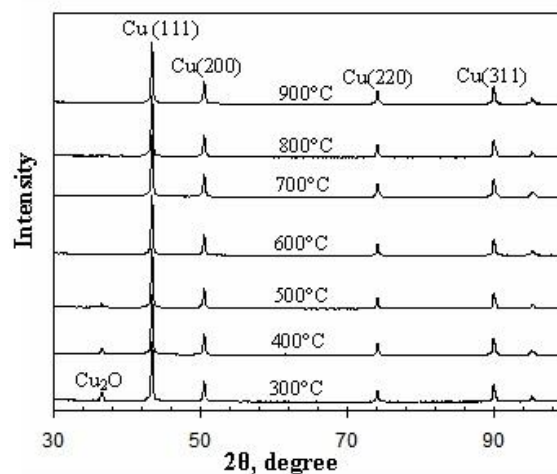
The detailed analysis of the IR spectra of Cu/C nanocomposites makes it possible to establish the nature of the surface of the carbon carriers obtained in the thermal decomposition reaction. The spectra of the CuC-H2-t samples are shown in Fig. 7. They have a low intensity of absorption bands, which is due to the carbonization of the fulvate residue, that already occurs at 300 °C. IR spectra of nanocomposites obtained at different temperatures have a similar form. The broad strong absorption band at about 3400 cm^{-1} can be attributed to the stretching vibrations of OH groups, which can be located on the surface of the carbon substrate or be a part of sorbed water. The presence of water is evidenced by an absorption band at about 1600 cm^{-1}, which corresponds to the bending vibrations of H_2O molecules. At the same time, the band of the stretching vibration of the C=O group at 1750–1730 cm^{-1}, characteristic for

acids, is not observed in the spectrum, which indicates a high degree of the fulvate residue conversion. The absorption bands at 2925 cm^{-1} and 2850 cm^{-1} correspond to the stretching vibrations, and 1400 cm^{-1} to the deformation vibrations of the CH bond, and the band at about 1410 cm^{-1} to the deformation vibrations of the O-H group bound to the phenolic ring.

The broad absorption band at about 1080 cm^{-1} with high intensity is due to stretching vibrations of the Cu – C bond, similar to those in copper (I) acetelenides [21].

Fig. 7. IR spectra of the decomposition products of copper (II) fulvate in the hydrogen atmosphere at different temperatures: 300 °C (a), 500 °C (b), 900 °C (c)

Fig. 8. Diffraction patterns of Cu/C nanocomposites obtained at different temperatures in inert atmosphere

Table 2

Sizes of copper nanoparticles in Cu/C nanocomposites, obtained at different temperatures in the inert atmosphere

Sample	Sizes of nanocrystallites calculated by the Scherrer formula (± 1), nm	Lattice parameter (a), (± 0.01) Å
Cu, bulk	–	3.6150
CuC-Ar-300	40	3.6156
CuC-Ar-400	44	3.6156
CuC-Ar-500	46	3.6156
CuC-Ar-600	49	3.6156
CuC-Ar-700	49	3.6156
CuC-Ar-800	52	3.6156
CuC-Ar-900	52	3.6252

The effect of the copper (II) humate decomposition reaction temperature in an inert atmosphere on the composition and structural properties of the obtained Cu/C nanocomposites was also investigated. Heating at a temperature above 300 °C leads to the reduction of copper. The fcc phase of copper was identified from the signals in the diffraction patterns (Fig. 8). Signals on the diffraction patterns are broadened, indicating the nanocrystalline copper content in the samples. The average sizes of nanoparticles calculated by the Schererr formula are 40–52 nm (Table 2).

With an increase in the reaction temperature from 300 to 900 °C, the size of nanoparticles increases due to the increase in their growth rate.

The weaker reducing properties of humate in comparison with hydrogen cause incomplete reduction of copper at heated to 300–500 °C, as a result, the signals from the Cu_2O (111) plane are observed in the diffractograms of these samples. Pyrolysis at high temperatures makes it possible to obtain nanocomposites that do not contain copper (II) oxide.
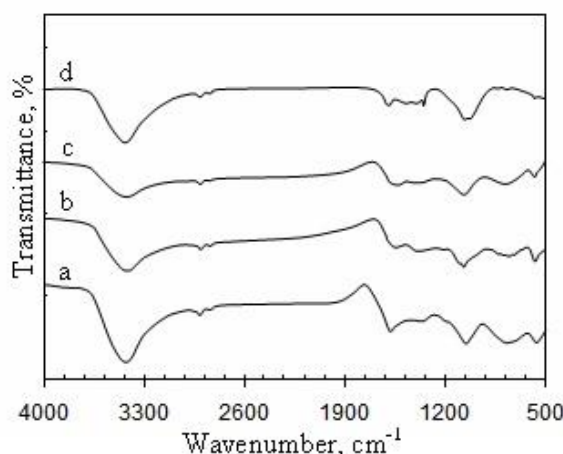

Fig. 9. IR spectra of the decomposition products of copper (II) fulvate at different temperatures in the inert atmosphere of 300°C (a), 500°C (b), 700°C (c), 900°C (d).

Similarly to the samples obtained in a hydrogen atmosphere, a wide and diffuse reflection peak from the graphite-like phase with a low intensity is observed on diffractograms Cu-Ar-300 in the range of angles $2\theta = 25–30°$ (Fig. 8). This indicates the presence of a turbo-strained structure. The increase of the reaction temperature causes a decrease in the reflection intensity in this region. It can be caused by a decrease in the amount of carbon in the nanocomposites due to its thermal decomposition, and is not observed for the samples obtained in a hydrogen atmosphere.

The IR spectra of the CuC-Ar-t samples (Fig. 9) exhibit bands similar to the samples obtained in a hydrogen atmosphere, indicating a similar nature of the surface groups on the carbon substrates of both series of samples.

Sorption properties of Cu/C nanocomposites. According to the data of nitrogen adsorption (Fig. 10), Cu/C nanocomposite obtained in a reducing atmosphere at 300 °C, preferably have a mesoporous structure. This means that the values of volume and specific surface area of micropores are significantly lower than the corresponding data for mesopores (Table 3)
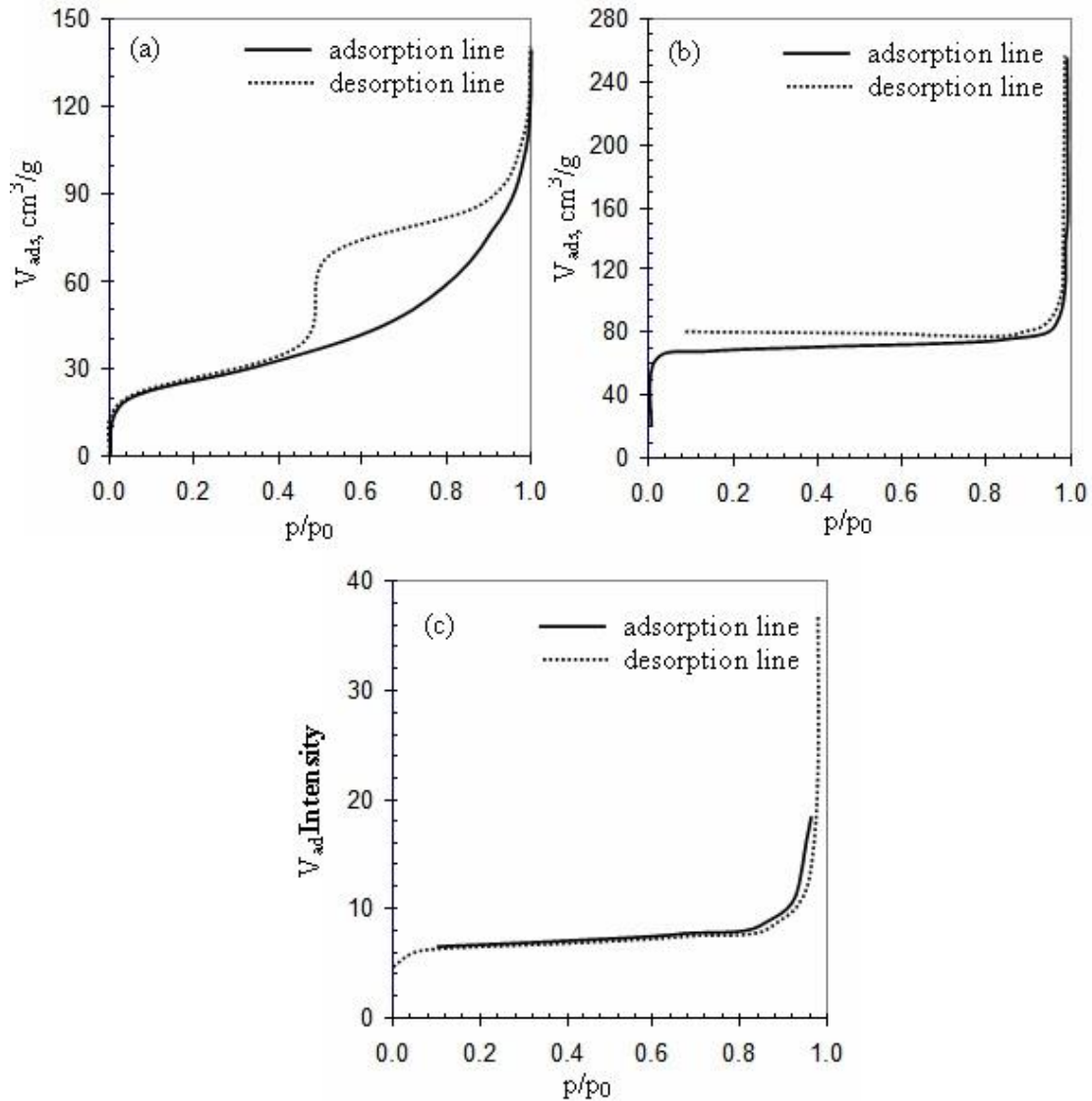
Fig. 10. Isotherms of ad(de)sorption of nitrogen by Cu/C nanocomposites: CuC-H₂-300 (a), CuC-H₂-700 (b), and CuC-Ar-500 (c)

The wide hysteresis observed on the isotherm (up to $p/p_s = 0.5$) can indicate the presence of either bottle-like mesopores, in which the diameter of the cavities is more than twice that the diameter of the inlets, or open slotted mesopores. In addition, the presence of a hysteresis loop can also be a consequence of the rupture of the meniscus (the tensile strength of nitrogen at rupture corresponds to $p/p_s = 0.5$), so the sample can be monoporous. The specific surface area (SBET) calculated by the Brunauer-Emmett-Teller (BET) method [17] is 96 m²/h.

Pyrolysis at high temperatures leads to the formation of materials with a microporous structure. The adsorption data for the CuC-H₂-700 sample indicate a significant increase of the volume of micropores with a simultaneous decrease in the part of mesopores. Accordingly, an increase of the specific surface area to 282 m²/g is observed. It can be assumed that heating the precursor to high temperatures leads to the collapse of the mesoporous structure and the formation of micropores in the process of further carbonization.

Table 3

Adsorption and structural characteristics (N₂, 77 K) of Cu/C nanocomposites

Sample	S_{BET}, m²/g	V_Σ, cm³/g	V_{meso}, cm³/g	D_{meso}, nm	V_{micro}, cm³/g	D_{micro}, nm
CuC-H₂-300	96	0.17	0.16	4.12	0.01	0.61
CuC-H₂-700	282	0.14	0.03	-	0.11	0.58
CuC-Ar-500	27	0.01	-	-	0.01	0.64

According to the adsorption data, the Cu/C nanocomposite obtained in an argon atmosphere has a microporous structure with a significantly lower total pore volume (Table 3), which is primarily due to a significantly lower carbon content in this sample compared to the previous one (35% compared to 50%). With a decrease in the pore volume, a corresponding decrease in the specific surface of the sample to 27 m^2/g is observed.

Conclusion

The copper nanoparticles in the amorphous carbon matrix were obtained by solid-phase pyrolysis of copper(II) humate in a reducing (H_2) and inert (Ar) atmosphere. Copper(II) humate was obtained by precipitation from a solution of synthetic sodium humate by Cu^{2+} ions. In the synthesis temperature range from 300 to 900 °C the size of metal particles in the nanocomposite increases from 40 to 80 nm. The detailed analysis of the IR spectra made it possible to establish the formation of the corresponding intermediate products at various stages of the nanocomposite preparation process. Pyrolysis of copper (II) humate in a reducing atmosphere of H_2 makes it possible to almost completely eliminate the oxygen present in synthetic humic substances from the final product, partly in the form of CO_2, and partly as water. Transition metal ions under these conditions are reduced to metal atoms, which form nanoparticles surrounded by a spatial network of linear and cyclic carbon blocks chaotically connected into a rigid structure. Thermal decomposition in a hydrogen atmosphere ensures the complete reduction of Cu^{2+} ions to Cu^0 and the retention of the maximum amount of carbon (about 50 %). The proposed method makes it possible to obtain a coating that is resistant to oxidation, and the polyfunctionality of synthetic humic substances ensures a uniform distribution of nanoparticles in the copper-carbon nanocomposites. Pyrolysis in the inert atmosphere leads to the formation of the copper oxides, in addition to the copper nanoparticles, and the carbon content does not exceed 35 %. The sorption properties of nanocomposites depend on the synthesis conditions. In particular, with an increase of temperature from 300 to 900 °C the structure of the nanocomposite changes from mesoporous to microporous. In addition, the increase of the pyrolysis temperature in a hydrogen atmosphere leads to the increase in the specific surface area of the obtained material from 96 to 282 m^2/g.

Bibliography

[1] Zaporotskova I. A. Metal–carbon nanocomposites based on pyrolysed polyacrylonitrile / I. A. Zaporotskova, L. V. Kozhitov, N. A.Anikeev, O. A.Davletova, A. V. Popkova, D. G. Muratov, E. V.Yakushko // Mod. Electron. Mater. – 2015. – Vol. 1 (2). – P. 43–49.

[2] Kryazhev Yu. G. Synthesis of metal–carbon nanocomposites containing nanoparticles of transition metals encapsulated in a graphite-like shell / Yu. G. Kryazhev, E. S. Zapevalova, O. N. Semenova, M. V. Trenikhin, V. S. Solodovnichenko, B. A. Likholobov // Protection of Metals and Physical Chemistry of Surfaces. – 2017. – Vol. 53. – P. 268–271.

[3] Kozhitov L.V. The Structureand Magnetic Properties Metal-carbon Nanocomposites NiCo/Con Based of Polyacrylonitrile / L.V. Kozhitov, D.G. Muratov, S.G. Emelyanov, V.G. Kostishin, E.V. Yakushko, A.G. Savchenko, I.V. Schetinin, E.P. Mosyakina // J. Nano-Electron. Phys. – 2014. – Vol. 6, No 3. – P. 03040.

[4] Fan R. Highly Dispersed Copper Nanoparticles Supported on Activated Carbon as an Efficient Catalyst for Selective Reduction of Vanillin / R. Fan, C. Chen, M. Han, W. Gong, H. Zhang, Y. Zhang, H. Zhao, G. Wang // Small. – 2018. – Vol. 14(36). – P.1801953.

[5] Gawande M.B. Cu and Cu-based nanoparticles: synthesis and applications in catalysis / M.B. Gawande, A. Goswami, F.X. Felpin // Chem Rev. – 2016. – Vol. 116. – P. 3722–3811.

[6] [6] Moeinzadeh S. Nanoparticles and their applications / S. Moeinzadeh, E. Jabbari // Springer, Berlin, 2017, P. 335–361.

[7] Ghoto S. A. Applications of copper nanoparticles for colorimetric detection of dithiocarbamate pesticides / S. A. Ghoto, M. Y. Khuhawar, T. M. Jahangir J. D. Mangi // J. Nanostruc. Chem. – 2019. – Vol. 9. – P. 77–93.

[8] Tabassum H. Recent advances in confining metal-based nanoparticles into carbon nanotubes for electrochemical energy conversion and storage devices / H. Tabassum, A.Mahmood, B. Zhu, Z. Liang, R. Zhong, S. Guo and R. Zou // Energy Environ. Sci. – 2019. – P. 1-98.

[9] Bocarando-Chacón J. Surface-enhanced Raman scattering and antibacterial properties from copper nanoparticles obtained by green chemistry / J. Bocarando-Chacón, D. Vargas-Vazquez, F. Martinez-Suarez, C. Flores-Juárez, M. Cortez-Valadez // Applied Physics A. – 2020. – Vol. 126. – P. 530.

[10] Shad A.A. Review of green synthesis and antimicrobial efficacy of copper and nickel nanoparticles / A.A. Shad // Am. J. Biomed. Sci. Res. – 2019. – Vol. 3(6). – P. 472–475.

[11] Singh A. An overview of processing and properties of Cu/CNT nano composites / A. Singh, T. Ram Prabhu, A.R.

Sanjay, V. Koti // Mater. Today Proc. **–** 2017. – Vol. 4. – P. 3872-3881.

[12] Li J. Carbon-coated copper nanoparticles: synthesis, characterizationand optical properties / J. Li, C. Liu // New J. Chem. – 2009. – Vol. 33. – P. 1474–1477.

[13] Huang Z. Direct observation of the formation andstabilization of metallic nanoparticles on carbonsupports / Z. Huang, Y. Yao, Z. Pang, Y. Yuan, T. Li, K. He, X. Hu, J. Cheng, W. Yao, Y. Liu, A. Nie, S. Sharifi-As,M. Cheng, B. Song, K. Amine, J. Lu, T. Li, L. Hu, R. Shahbazian-Yassar // Nat. commun. – 2020. – Vol. 11 (6). – P. 6373.

[14] Sehaqui H. Facile and universal method for the synthesis of metal nanoparticles supported onto carbon foams / H. Sehaqui, Y. Brahmi, W. Ju // Cellulose. **–** 2020. **–** Vol. 27. **–** P.263–271.

[15] Seo J. Y. One-step synthesis of copper nanoparticles embedded in carbon composites / J. Y. Seo, H. W. Kang, D. S. Jung, H. M. Lee, S. BinPark // Mater. Res. Bull. – 2013. – Vol. 48 (4). – P. 1484-1489

[16] Litvin V.A. Synthetic fulvic acids from tannin / V. A. Litvin, R. Abi Njoh // Journal of Chemistry and Technologies. – 2020. – 28(3). – 251-259.

[17] Gregg S.G. Adsorption, surface area and porosity / S.G. Gregg, K.S.W. Sing, 2nd Edition edn. Academic press, London, 1982. – 303 p.

[18] Horvath G. Method for calculation of effective pore size distribution in molecular sieve carbon / G. Horvath, K. Kawazoe // J.Chem. Eng. Jpn. – 1983. – Vol. 16. – P. 470–475.

[19] [19] Yang T. The copper complexation ability of a synthetic humic-like acid formed by an abiotic humification process and the effect of experimental factors on its copper complexation ability / T. Yang, M. E. Hodson // Environ. Sci. Pollut. Res. – 2018. – Vol. 25. – P. 15873–15884.

[20] Gomes de Melo B. A. Humic acids: Structural properties and multiple functionalities for novel technological developments / B. A. Gomes de Melo, F. L. Motta, M. H. Santana // Mater Sci Eng C. – 2016. – Vol. 62. – P. 967–974.

[21] Litvin, V.A. Synthesis and properties of synthetic fulvic acid derived from hematoxylin / V.A. Litvin, B.F. Minaev, G.V. Baryshnikov // J. Mol. Struct. – 2015. – Vol. 1086. – P. 25–33.

[22] Machadoa W. Spectroscopic characterization of humic and fulvic acids in soil aggregates / W. Machadoa, J. C. Franchini, M. de Fátima Guimarães, J.T. Filho // Brazil. Heliyon. – 2020. – Vol. 6(6). – P. 04078.

[23] Theivasanthi T. X-Ray Diffraction Studies of Copper Nanopowder / T. Theivasanthi, M. Alagar // Arch. Phys. Res. – 2010. – Vol. 1 (2). – P. 112-117.

[24] Afolabi A. S. Synthesis of carbon nanotubes and nanoballsby swirled floating catalyst chemicalvapour deposition method / A. S. Afolabi, A. S. Abdulkareem, S. E. Iyuke // J. Exp. Nanosci. – 2007. – Vol. 2 (4). – P. 269–277.

References

[1] Zaporotskova, I. A., Kozhitov, L. V., Anikeev, N. A., Davletova, O. A., Popkova, A. V., Muratov, D. G., Yakushko, E. V. (2015). Metal–carbon nanocomposites based on pyrolysed polyacrylonitrile. *Mod. Electron. Mater.*, *1* (2), 43-49. https://doi.org/10.1016/j.moem.2015.11.004

[2] Kryazhev, Yu. G., Zapevalova, E. S., Semenova, O. N., Trenikhin, M. V., Solodovnichenko, V. S., Likholobov, B. A. (2017). Synthesis of metal–carbon nanocomposites containing nanoparticles of transition metals encapsulated in a graphite-like shell. *Protection of Metals and Physical Chemistry of Surfaces*, *53*, 268–271. https://doi.org/10.1134/S2070205117020150

[3] Kozhitov, L.V., Muratov, D.G., Emelyanov, S.G., Kostishin, V.G., Yakushko, E.V., Savchenko, A.G., Schetinin, I.V., Mosyakina, E.P. (2014). The Structureand Magnetic Properties Metal-carbon Nanocomposites NiCo/C on Based of Polyacrylonitrile. *J. Nano- Electron. Phys.*, *6* (3), 03040.

[4] Fan R., Chen, C., Han, M., Gong, W., Zhang, H., Zhang, Y., Zhao, H., Wang, G. (2018) Highly Dispersed Copper Nanoparticles Supported on Activated Carbon as an Efficient Catalyst for Selective Reduction of Vanillin. *Small, 14*(36), 1801953. https://doi.org/10.1002/smll.201801953

[5] Gawande, M.B., Goswami, A., Felpin F.X. (2016). Cu and Cu-based nanoparticles: synthesis and applications in catalysis. *Chem. Rev.*, *116*, 3722–3811. https://doi.org/10.1021/acs.chemrev.5b00482

[6] Moeinzadeh, S., Jabbari, E. (2017). Nanoparticles and their applications Springer, Berlin, 2017, P. 335–361. https://doi.org/10.1007-/978-3-662-54357-3_11

[7] Ghoto, S. A., Khuhawar, M. Y., Jahangir, T. M., Mangi, J. D. (2019) Applications of copper nanoparticles for colorimetric detection of dithiocarbamate pesticides. *J. Nanostruc. Chem.*, *9*, 77–93. https://doi.org/10.1007/s40097-019-0299-4

[8] Tabassum, H., Mahmood, A., Zhu, B., Liang, Z., Zhong, R., Guo, S., Zou, R. (2019). Recent advances in confining metal-based nanoparticles into carbon nanotubes for electrochemical energy conversion and storage devices. *Energy Environ. Sci.*, 1-98. https://doi.org/10.1039/C9EE00315K

[9] Bocarando-Chacón, J., Vargas-Vazquez, D., Martinez-Suarez, F., Flores-Juárez, C., Cortez-Valadez, M. (2020) Surface-enhanced Raman scattering and antibacterial properties from copper nanoparticles obtained by green chemistry. *Applied Physics A. 126*, 530. https://doi.org/10.1007/s00339-020-03704-1

[10] Shad, A.A. (2019) Review of green synthesis and antimicrobial efficacy of copper and nickel nanoparticles. *Am. J. Biomed. Sci. Res.*, *3*(6), 472–475. 10.34297/AJBSR.2019.03.000721

[11] Singh, A, Ram Prabhu, T, Sanjay, AR, Koti V. (2017). An overview of processing and properties of Cu/CNT nano composites. *Mater. Today Proc.*, *4*, 3872-3881. https://doi.org/10.1016/j.matpr.2017.02.286

[12] Li, J., Liu, C. (2009) Carbon-coated copper nanoparticles: synthesis, characterizationand optical properties. *New J. Chem.*, *33*, 1474–1477. https://doi.org/10.1039/B906796E

[13] Huang, Z., Yao, Y., Pang, Z., Yuan, Y., Li, T., He, K., Hu, X., Cheng, J., Yao, W., Liu, Y., Nie, A., Sharifi-As, S., Cheng, M., Song, B., Amine, K., Lu, J., Li, T., Hu, L., Shahbazian-Yassar R. (2020) Direct observation of the formation andstabilization of metallic nanoparticles on carbonsupports. *Nat. commun.*, *11* (6), 6373. https://doi.org/10.1038/s41467-020-20084-5

[14] Sehaqui, H., Brahmi, Y., Ju, W. (2020) Facile and universal method for the synthesis of metal nanoparticles supported onto carbon foams. *Cellulose*, *27*, 263–271. https://doi.org/10.1007/s10570-019-02805-2

[15] [15] Seo, J. Y., Kang, H. W., Jung, D. S., Lee, H. M., BinPark, S. (2013) One-step synthesis of copper nanoparticles embedded in carbon composites. *Mater. Res. Bull.*, *48 (4)*, 1484-1489. https://doi.org/10.1016/j.materresbull.2012.12.070

[16] Litvin, V.A., Abi Njoh, R. (2020) Synthetic fulvic acids from tannin. *Journal of Chemistry and Technologies*, *28*(3), 251-259. https://doi.org/10.15421/082027

[17] Gregg, S.G., Sing, K.S.W. (1982) Adsorption, surface area and porosity, 2nd Edition edn. Academic press, London, 1982.

[18] Horvath, G., Kawazoe, K. (1983) Method for calculation of effective pore size distribution in molecular sieve carbon. *J. Chem. Eng. Jpn.*, *16*, 470–475. https://doi.org/10.1252/jcej.16.470

[19] Yang, T., Hodson, M. E. (2018) The copper complexation ability of a synthetic humic-like acid formed by an abiotic humification process and the effect of experimental factors on its copper complexation ability. *Environ. Sci. Pollut. Res.*, *25*, 15873–15884. https://doi.org/10.1007/s11356-018-1836-2

[20] Gomes de Melo, B. A., Motta, F. L., Santana, M. H. (2016) Humic acids: Structural properties and multiple functionalities for novel technological developments. *Mater Sci Eng C.*, *62*, 967–974. https://doi.org/10.1016/j.msec.2015.12.001

[21] Litvin, V.A., Minaev, B.F., Baryshnikov, G.V. (2015) Synthesis and properties of synthetic fulvic acid derived from hematoxylin. *J. Mol. Struct.*, *1086*, 25–33. https://doi.org/10.1016/j.molstruc.2014.12.091

[22] Machadoa W., Franchini J. C., de Fátima Guimarães M., Filho J.T. (2020) Spectroscopic characterization of humic and fulvic acids in soil aggregates. *Brazil. Heliyon, 6(6)*, 04078. https://doi.org/10.1016/j.heliyon.2020.e04078

[23] Theivasanthi, T., Alagar, M. (2010) X-Ray Diffraction Studies of Copper Nanopowder. *Arch. Phys. Res.*, 1 (2), 112-117.

[24] Afolabi, A. S., Abdulkareem, A. S., Iyuke, S. E. (2007) Synthesis of carbon nanotubes and nanoballsby swirled floating catalyst chemicalvapour deposition method. *J. Exp. Nanosci.*, *2* (4), 269–277. https://doi.org/10.1080/17458080701745658